

# Stripe orders driven by long-range Coulomb forces in the 2D-Hubbard model

R. Citro<sup>a</sup> and M. Marinaro

Dipartimento di Fisica "E.R. Caianiello", University of Salerno and Unità INFN of Salerno, Baronissi (Sa), Italy

Received 20 November 2000

**Abstract.** Within the single band 2D-Hubbard model treated by means of a strong-coupling approach based on a cumulant expansion and a nonstandard diagrammatic technique, we discuss the existence of critical charge fluctuations that could give rise to an instability towards a phase separation (PS). It turns out that such instability exists and evolves into an incommensurate charge density wave (ICDW) when long-range Coulomb forces are taken into account. We find a stripe phase with a crossover from diagonal to vertical stripes at increasing doping in the range  $0.01 \leq \delta \leq 0.2$  and increasing Coulomb potential  $U$ , similarly to recent NMR experiments on  $\text{La}_{2-x}\text{Sr}_x\text{CuO}_4$ .

**PACS.** 71.10.Fd Lattice fermion models (Hubbard model, etc.) – 71.45.Lr Charge-density-wave systems – 71.27.+a Strongly correlated electron systems; heavy fermions

## 1 Introduction

The basic issue in the study of the high- $T_c$  superconductors is related to the understanding of the anomalous behavior in the normal phase characterized by the breakdown of the conventional Fermi-liquid description. The major features signaling the non conventional character of the metallic phase come from the optical conductivity [1], electrical resistivity [2,3] and angle resolved photoemission experiments [4–6]. It is widely believed that the failure of the Fermi-liquid theory in the metallic phase of the cuprates has to be ascribed to a singular interaction among the electrons that manifests near some quantum critical point (QCP) at zero temperature [7–9]. Within this scenario the singular scattering induced by critical fluctuations would be responsible for the anomalous normal-state properties. Different realizations of such scenario ascribe the origin of the singular interaction to a phase separation (PS), to a spin density wave in proximity of an antiferromagnetic AF-QCP [7,8], or a charge density wave in proximity of an incommensurate charge density wave ICDW-QCP [9]. The theories based on the AF-QCP [7,8] rely on the existence of an antiferromagnetic phase in the low doping region and the observation of strong spin fluctuations at larger doping [10,11]. On the other hand, recent experimental results support the existence of a QCP near optimal doping involving charge degrees of freedom [12,13]. As suggested by the experiments in  $\text{La}_{2-x}(\text{NdSr})_x\text{CuO}_4$  [14], near and above optimum doping the spin degrees of freedom are enslaved in the proximity of the ICDW-QCP where a stripe-phase

takes place. Coexistence of ICDW and electron gas has been observed in joint EXAFS [15] and X-ray diffraction [16] experiments. Also the recent experiments based on neutron powder diffraction measurements of the atomic pair distribution function [13] in  $\text{La}_{2-x}\text{Sr}_x\text{CuO}_4$ , over the range of doping  $0.0 \leq x \leq 0.30$  at low temperature, show a broadening of the in-plane Cu–O bond distribution at increasing doping indicating the presence of charge inhomogeneities in the  $\text{CuO}_2$  plane, while a sharpening of the peak is detected just above optimum doping suggesting a crossover to an homogeneous metal. These experimental evidences reveal that optimum doping emerges as a peculiar point in the phase diagram of cuprates, not only associated to the highest  $T_c$ , but also connected to the crossover in the normal state properties, as suggested by the ICDW-QCP scenario [9].

The aim of the present paper is to give a microscopic description for the occurrence of a QCP in the proximity of a charge instability. We investigate the existence of a such instability in the single-band Hubbard model treated by means of a strong-coupling approach based on a cumulant expansion and a nonstandard diagrammatic technique. The approach makes use of a *non-Fermi liquid* description of the single-band Hubbard model and in this scheme the charge vertex at low energy as a function of the doping is analyzed within a generalized random phase approximation (RPA). We find that the vertex becomes singular tuning the doping. The singularity appears at the wave-vector  $\mathbf{k} = 0$ , as expected due to absence of long-range order forces in the model. When long-range Coulomb forces are taken into account, the competition between phase separation and long-range repulsive forces gives rise to an incommensurate CDW scattering

---

<sup>a</sup> e-mail: citro@sa.infn.it

near some finite vector  $\mathbf{k}_c$ . We thus recover the result obtained in references [9] by the use of a standard large- $N$  approach within the Hubbard-Holstein model. The CDW fluctuations mediate a strong momentum-dependent effective interaction among electrons which could be responsible for a pseudogap formation in the spectral density caused by dynamical charge modulations.

The paper is organized as follows. In Section 2 the model and the general formalism are presented. Section 3 contains the analysis of the charge vertex function and its low-energy behavior in presence of the local Coulomb repulsion only. In Section 4 we generalize our approach to take into account long-range Coulomb forces and finally draw the conclusions in Section 5.

## 2 Formalism

We write the single-band Hubbard Hamiltonian as  $H = H_0 + H_I$ , where  $H_0 = \sum_i H_i^0$  is the atomic Hamiltonian with

$$H_i^0 = -\mu \sum_{\sigma} n_{i\sigma} + U n_{i\uparrow} n_{i\downarrow} \quad (1)$$

$$H_I = \sum_{\langle i,j \rangle, \sigma} t_{ij} c_{i\sigma}^{\dagger} c_{j\sigma}, \quad (2)$$

$c_{i\sigma}^{\dagger} (c_{i\sigma})$  is an electron creation (annihilation) operator with spin  $\sigma$  at site  $i$ .  $U$  is the Coulomb repulsion,  $\mu$  the chemical potential and  $t_{ij}$  denotes the nearest neighbor hopping. Since the zeroth order Hamiltonian contains the Coulomb interaction, it can be diagonalized by using the Hubbard and not the free electron operators. As a consequence the ordinary Wick's theorem in the evaluation of chronological averages is not valid. Instead a generalized Wick's theorem has been proposed that permits to evaluate the one-particle Matsubara Green functions by means of a nonstandard diagram technique [17–19].

In a previous work we have calculated the one-particle Green's function by considering only chain-type of diagrams [20] which take into account first order cumulants. This approximation leads to the Hubbard I type Green's function  $G^{(1)}(\mathbf{k}, i\omega_n)$ , in which the energy spectrum consists of two Hubbard subbands,

$$G_{\sigma}^{(1)}(\mathbf{k}, i\omega_n) = \frac{G_{\sigma}^{(0)}(i\omega_n)}{1 - t(\mathbf{k})G_{\sigma}^{(0)}(i\omega_n)} = \sum_{i=1,2} \frac{A_i(\mathbf{k})}{i\omega_n - \varepsilon_i(\mathbf{k})}, \quad (3)$$

where  $G_{\sigma}^{(0)}(i\omega_n)$  is the local-Hubbard Green's function,  $\varepsilon_i(\mathbf{k})$  is the energy band dispersion,  $A_i(\mathbf{k})$  are the spectral weights of the two subbands,  $t(\mathbf{k})$  is the Fourier transform of the hopping term. Their explicit expressions are the following:

$$G_{\sigma}^{(0)}(i\omega_n) = \frac{1 - \langle n_{-\sigma} \rangle}{i\omega_n - \mu} + \frac{\langle n_{-\sigma} \rangle}{i\omega_n - (U - \mu)}, \quad (4)$$

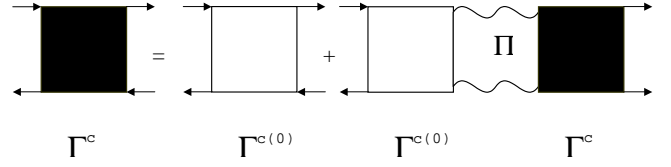


**Fig. 1.** Bethe-Salpeter equation for the vertex function  $\Gamma^c$  in the particle-hole channel. The thin wavy-line represents the renormalized hopping.

where  $\langle n_{-\sigma} \rangle$  is the averaged on-site density of electrons with spin  $-\sigma$ ,

$$\varepsilon_{1,2}(\mathbf{k}) = \frac{1}{2} \left[ (U - 2\mu) + t(\mathbf{k}) \mp \sqrt{(U - t(\mathbf{k}))^2 + 4t(\mathbf{k})\langle n_{-\sigma} \rangle} \right], \quad (5)$$

where  $t(\mathbf{k}) = -2t(\cos k_x + \cos k_y)$ ,

$$A_1(\mathbf{k}) = \frac{\varepsilon_1(\mathbf{k}) - U(1 - \langle n_{-\sigma} \rangle)}{\varepsilon_1(\mathbf{k}) - \varepsilon_2(\mathbf{k})} = 1 - A_2(\mathbf{k}). \quad (6)$$

Besides, we have calculated the two-particle Green's functions, *i.e.* some generalized susceptibilities [21], by introducing second order cumulants. Here we consider a *charge dressed vertex* obtained from the summation of a special class of irreducible diagrams in the particle-hole channel, *i.e.* the ladder-type of diagrams shown in Figure 1, which takes into account two-particle correlation effects. For the vertex we use a square diagram to remember that it corresponds to a local average of four operators. In the weak-coupling theory the summation of diagrams of type (7) is known as Random Phase Approximation (RPA). The difference between the weak-coupling RPA and our ladder generalized RPA is contained in the bare vertex parts, which are not given by bare potentials but two-particles cumulants connected by a renormalized hopping.

The charge vertex obeys the following Bethe-Salpeter equation

$$\Gamma^c(\mathbf{k}, i\omega_n) = \Gamma^c(0)(i\omega_n) + \Gamma^c(0)(i\omega_n)\Pi(\mathbf{k}, i\omega_n)\Gamma^c(\mathbf{k}, i\omega_n). \quad (7)$$

$\Gamma^c(0)$  is the bare interaction vertex function that in our case is a two-particle cumulant, *i.e.* a local two-particle irreducible Green's function, whose expression has been calculated following the method of reference [22]:

$$\Gamma^c(0)(i\omega_n) = \langle n_{\sigma} \rangle^2 \left[ \frac{1}{i\omega_n + U} - \frac{1}{i\omega_n - U} \right], \quad (8)$$

$\Pi(k)$  is the polarization insertion given by

$$\Pi(k) = -2t(\mathbf{k}) - \frac{2}{\beta} \sum_{q, \sigma} t^2(\mathbf{k} + \mathbf{q}) t^2(\mathbf{q}) G_{\sigma}^{(1)}(k + q) G_{\sigma}^{(1)}(q). \quad (9)$$

Here we have introduced the shorthand notation  $k = (\mathbf{k}, i\omega_n)$  and similarly for  $q$ .

Within Green's function formalism, the instabilities driven by charge fluctuations are signaled by the poles of the vertex function  $\Gamma^c$  (at zero temperature). Next, we study the vertex function in the total frequency variable to investigate the possible proximity of the system to a criticality.

### 3 The charge-vertex function

In the following it is assumed that we start from the phase where there is no order parameter and study the charge vertex. When this function is singular, it is an indication that a phase separation (when  $k \rightarrow 0$ ) or a charge ordering (CDW) at finite  $k$  occurs in the system. To start with, we perform the analytical continuation in equation (7) and write the charge vertex as

$$\Gamma^c(\mathbf{k}, \omega) = \frac{1}{[\Gamma^c(0)(\omega)]^{-1} - \text{Re}\Pi(\mathbf{k}, \omega) - i\text{Im}\Pi(\mathbf{k}, \omega)}. \quad (10)$$

Numerical results show a deep minimum of the real part of  $[\Gamma^c(\mathbf{k}, \omega)]^{-1}$  at the wave vector  $\mathbf{k} = 0$  at small frequencies. In this region we analyze the real and the imaginary part of the denominator in (10), separately. In the range of values of  $U$  of interest, the real part has been calculated numerically. A good fitting of such part is given by the function  $-\Omega(\mathbf{k})$ , where:

$$\Omega(\mathbf{k}) = (U + 4t(\mathbf{k})\langle n_\sigma \rangle^2)/2\langle n_\sigma \rangle^2. \quad (11)$$

The expansion around  $\mathbf{k} = 0$  gives

$$\Omega(\mathbf{k}) \simeq m(\delta) + \alpha\mathbf{k}^2, \quad (12)$$

where  $m(\delta)$  is the mass term. It is a function of the doping  $\delta = (1 - 2\langle n_\sigma \rangle)$  and vanishes in correspondence of the critical value [21]  $\langle n_\sigma^c \rangle = \sqrt{U}/8$ , where  $U$  is expressed in units of  $t$ . In particular, it can be easily shown that the mass term is linearly vanishing by approaching  $\delta_c$ , *i.e.*  $m \simeq (8/\langle n_\sigma^c \rangle)(\delta - \delta_c)$ .

The analysis of the imaginary part is more involved and takes much care. In the small  $\omega$  limit, the analytical results show that  $\text{Im}\Pi(\mathbf{k}, \omega)$  is linear in  $\omega$

$$\text{Im}\Pi(\mathbf{k}, \omega) \simeq -\gamma(\mathbf{k})\omega + O(\omega^2) \quad (13)$$

where  $\gamma(\mathbf{k})$  is the inverse of the relaxation time of the charge fluctuations. For small  $k$  we can extract the angular dependence of the relaxation time, *i.e.*

$$\gamma(\mathbf{k}) \simeq \frac{1}{|k|}\gamma(\phi), \quad (14)$$

where

$$\begin{aligned} \gamma(\phi) = & \frac{1}{4t^2} \frac{\pi V^4}{g(V)^2} \frac{U^2(1 - \langle n_\sigma \rangle)^2}{(U - V)^2 + 4UV\langle n_\sigma \rangle} \\ & \times \int_{-\pi}^{\pi} \frac{dq_x}{2\pi} \int_{-\pi}^{\pi} \frac{dq_y}{2\pi} \sqrt{1 + \tan^2(\phi)} \\ & \times \delta(\sin q_x + \tan(\phi) \sin q_y) \delta(\cos q_x + \cos q_y + \frac{V}{2t}), \end{aligned} \quad (15)$$

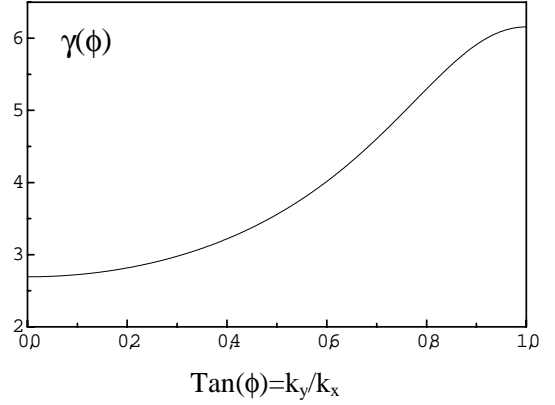


Fig. 2. Anisotropy of  $\gamma(\phi)$  for  $U/t = 5$  and  $\delta = 0.1$ .

$V = \frac{\mu(U-\mu)}{U-\mu-U\langle n_\sigma \rangle}$ ,  $g(V) = \frac{1}{2}(1 - \frac{U(2\langle n_\sigma \rangle - 1) + V}{\sqrt{(U-V)^2 + 4UV\langle n_\sigma \rangle}})$ ,  $\mu$  is the chemical potential which is determined in a self-consistent way together with the total number of particles,  $\tan \phi = k_y/k_x$ , and the lattice spacing has been put equal to one. As shown in Figure 2  $\gamma(\phi)$  is an anisotropic function in the  $\mathbf{k}$  space, that becomes maximum along the diagonal direction.

From equations (11) and (13) we deduce that in the low-energy region and for  $\mathbf{k} \rightarrow 0$  the charge vertex can be written as

$$\Gamma^c(\mathbf{k}, \omega) \simeq -\frac{1}{m(\delta) + \alpha\mathbf{k}^2 - i\gamma(\phi)\frac{\omega}{k}}. \quad (16)$$

This expression of  $\Gamma^c$  is consistent with that obtained by Di Castro *et al.* in the large-N expansion of the Hubbard-Holstein model [9]. As shown in equation (16),  $\Gamma^c$  is singular at  $\omega = 0$  when  $\mathbf{k} \rightarrow 0$  signaling the occurrence of a phase separation (PS) for a finite value of the doping. The existence of such singularity causes a singular scattering amplitude between quasiparticles with important consequences on the single-particle properties where the violation of the Fermi liquid behaviour mainly manifests through the transfer of spectral weight from the quasiparticle peak to an incoherent background. Besides, the anisotropy of the vertex can explain the different behavior of electrons or holes on the Fermi surface.

### 4 Effects of long-range Coulomb interaction

In this section we discuss the importance of the long-range Coulomb (LRC) forces that could provide the basic ingredient driving the system towards a charge aggregation. The question of the importance of LRC forces has already been addressed in some theoretical works [9,23]. Within a different approach applied to the Hubbard-Holstein model [9,24], the results showed that LRC forces render the scattering amplitude between quasiparticles *anisotropic* introducing an ordering in the system and rendering it similar to the case of magnetic fluctuations [8]. In our formalism, we would like to assess a similar electronic origin of an incommensurate CDW. As we have previously

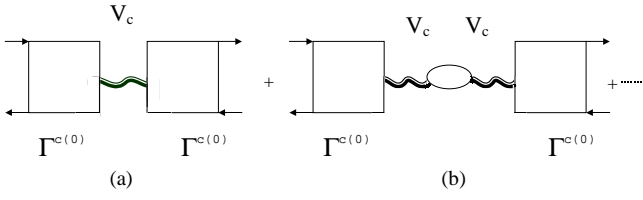


**Fig. 3.** New types of diagrams appearing when long-range Coulombic forces are taken into account. The thick wavy-line represents the Coulombic potential.

seen the generalized susceptibility and consequently the charge vertex  $\Gamma_c(\mathbf{q}, \omega)$  in our formalism, provide evaluable informations on the stability of the system. In particular, a divergence in the charge vertex  $\Gamma_c(\mathbf{q}, \omega = 0)$  signals the occurrence of a Phase Separation (PS) when  $q \rightarrow 0$  or a CDW when  $q$  is finite. In the absence of LRC forces the instability occurs at  $q = 0$  up to some intermediate doping. As we will see, the introduction of LRC forces eliminates the small- $q$  divergence in the static correlation function giving rise to a finite  $q$  instability. The long-range Coulomb interaction term is described by the following Hamiltonian

$$H_c = \sum_{i,j,\sigma} V_{ij} n_{i\sigma} n_{j\sigma}, \quad (17)$$

where  $n_{i\sigma} = c_{i\sigma}^\dagger c_{i\sigma}$  is the local density. It represents the Coulombic potential between the electrons on a two-dimensional square lattice embedded in a three-dimensional space with a separation  $d$  between the plane in  $z$ -direction. In the momentum space such Hamiltonian can be written as

$$H_c = V_c \sum_{\mathbf{q}} G(\mathbf{q}) \rho_{\mathbf{q}} \rho_{-\mathbf{q}}. \quad (18)$$

where  $\rho_{\mathbf{q}} = \sum_{\mathbf{k}, \sigma} c_{\mathbf{k}+\mathbf{q}, \sigma}^\dagger c_{\mathbf{k}, \sigma}$ ,  $V_c$  is the Coulombic coupling constant,  $G(\mathbf{q})$  is an anisotropic function in the momentum-space whose expression has been explicitly calculated in reference [24] by using a discretized form of the Laplace equation. Indicating with  $\varepsilon_{\parallel}$  and  $\varepsilon_{\perp}$  the dielectric constants in the plane and perpendicular to it, it was found that  $V_c = e^2 d / 2\varepsilon_{\perp} a^2$  and  $G(\mathbf{q}) = \frac{1}{\sqrt{A^2(\mathbf{q})-1}}$ , where  $A(\mathbf{q}) = [\varepsilon_{\parallel} / (\varepsilon_{\perp} a^2 / d^2)] [(\cos(aq_x) + \cos(aq_y)) - 2] - 1$ . In the following we assume the values of the parameters of a copper oxide superconductors of 214 type,  $d \simeq 3a$ ,  $\varepsilon_{\perp} \simeq 5$ ,  $\varepsilon_{\parallel} \simeq 30$ . Let us generalize our diagrammatic technique to the case when a LRC potential is included. Apart the diagrams shown in figure 1 a new series of diagrams has to be considered. They are shown in figure 3.

Within the previous approximation, we can sum these new sets of diagrams to obtain the following expression for the vertex function

$$\Gamma(\mathbf{k}, i\omega_n) = \frac{\Gamma^{c(0)}(i\omega_n) V(\mathbf{k}) \Gamma^{c(0)}(i\omega_n)}{1 - V(\mathbf{k}) \left( \tilde{\Pi}(\mathbf{k}, i\omega_n) + \Gamma^{c(0)}(i\omega_n) \right)}, \quad (19)$$

where  $V(\mathbf{k}) = V_c G(\mathbf{k})$ ,  $\tilde{\Pi}(\mathbf{k}, i\omega_n) = -\frac{2}{\beta} \sum_{q, \sigma} G_{\sigma}^{(1)}(k+q) G_{\sigma}^{(1)}(q)$ .

First, we neglect the subset of diagrams of type (b), *i.e.* the contribution from  $\tilde{\Pi}(\mathbf{k}, i\omega_n)$ . The total LRC vertex is expressed in terms of the short-range (SR) one, given by (7), through the following relation

$$\begin{aligned} \Gamma^{\text{LR}}(\mathbf{k}, i\omega_n) &= \frac{\Gamma^{c(0)}(i\omega_n)}{1 - \Gamma^{c(0)}(i\omega_n) (\Pi(\mathbf{k}, i\omega_n) + V(\mathbf{k}))} \\ &= \frac{\Gamma^{\text{SR}}(\mathbf{k}, i\omega_n)}{1 - \Gamma^{\text{SR}}(\mathbf{k}, i\omega_n) V(\mathbf{k})}. \end{aligned} \quad (20)$$

With our choice of diagrams, the expression for the LRC vertex in terms of the SR one is the same as that obtained in references [9]. After performing the analytical continuation, it can be seen that a divergence in  $\Gamma^{\text{SR}}(\mathbf{k}, \omega = 0)$  does not give a divergent response function at LR. Furthermore, since  $V_c / \sqrt{A^2(\mathbf{k}) - 1} \rightarrow \infty$  when  $\mathbf{k} \rightarrow 0$ , the compressibility should vanish as in a Coulomb gas and thus the instability to a PS is completely suppressed. New instabilities in the system can arise when

$$\Gamma^{c(0)}(\omega = 0)^{-1} - \Pi(\mathbf{k}, \omega = 0) = V_c / \sqrt{A^2(\mathbf{k}) - 1}. \quad (21)$$

The inclusion of the set of diagrams (b) can be performed, as usual, by introducing the renormalization of the bare potential  $V(\mathbf{k})$ . Indicating with  $V^{\text{R}}(\mathbf{k}, i\omega_n)$  the renormalized potential

$$V^{\text{R}}(\mathbf{k}, i\omega_n) = \frac{V(\mathbf{k})}{1 + V(\mathbf{k}) \tilde{\Pi}(\mathbf{k}, i\omega_n)}, \quad (22)$$

we obtain

$$\begin{aligned} \Gamma^{\text{LR}}(\mathbf{k}, i\omega_n) &= \frac{\Gamma^{c(0)}(i\omega_n)}{1 - \Gamma^{c(0)}(i\omega_n) (\Pi(\mathbf{k}, i\omega_n) + V^{\text{R}}(\mathbf{k}, i\omega_n))} \\ &= \frac{\Gamma^{\text{SR}}(\mathbf{k}, i\omega_n)}{1 - \Gamma^{\text{SR}}(\mathbf{k}, i\omega_n) V^{\text{R}}(\mathbf{k}, i\omega_n)}. \end{aligned} \quad (23)$$

In the rest of the paper we will neglect the contribution of diagrams of type (b) since the use of the renormalized potential is not essential to describe a finite- $k$  instability. An extensive numerical analysis of the equation (21) has been performed to search for the existence of a finite  $\mathbf{k}$  instability in the system. Equation (21) defines a line in the Brillouin Zone (BZ) given by the intersection of two surfaces (the first and second members of (21)) reported in Figure 4. The instability due to LRC effects appears at the point on the intersection line where  $V(\mathbf{k})$  takes the smallest value. The vector at which the instability occurs is denoted by  $\mathbf{k}_c$ . The dependence on  $U$  of  $\mathbf{k}_c$  is reported in Figure 5. The analysis of  $\mathbf{k}_c = (k_{cx}, k_{cy})$  shows that the larger values of  $U$  drive the instability close to the (1,0) or (0,1) direction. As  $U$  increases a transition from diagonal to vertical stripes is observed. This is a consequence of the structure of the short-range vertex function that is enhanced by the large density of states along the (1,0) or (0,1) direction. Besides, at increasing

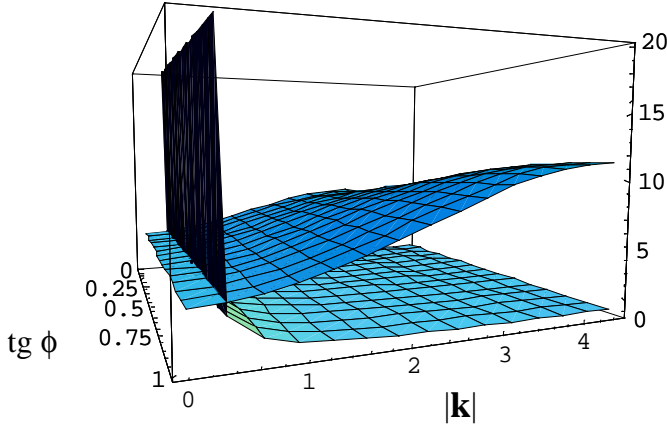


**Fig. 4.** Intersection of the two surfaces in equation (21) as a function of the modulus  $|\mathbf{k}|$  and the direction  $\text{tg}\phi$  for  $U = 6t$ ,  $V_c = 3t$ ,  $\delta = 0.1$ .

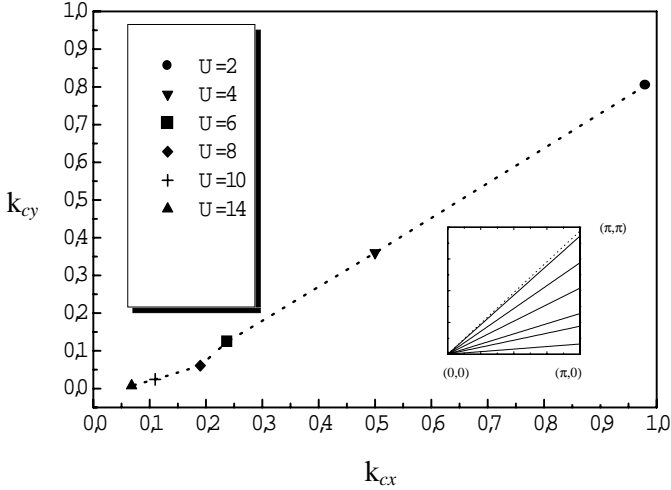


**Fig. 5.** Dependence of the components  $k_{cx}$  and  $k_{cy}$  at varying  $U$  in units of  $t$  for the other values of parameters as in Figure 4. The dashed line has no physical meaning. It is used to put in evidence the change in the direction of  $\mathbf{k}_c$  vs.  $U$ . The inset shows the direction normal to the stripes at increasing  $U$  starting from the diagonal.

$U \mathbf{k}_c \rightarrow (0,0)$  indicating that the local Coulomb repulsion is more effective in driving the systems towards a PS. The results as a function of the doping are plotted in Figure 6 and show that the effect of LRC forces is stronger in the low-doping region where the distance among the stripes ( $\propto \frac{1}{|\mathbf{k}_c|}$ ) is decreased. The dependence on  $\delta$  of the direction of the critical vector  $\mathbf{k}_c$  is reported in the inset of Figure 6. It becomes closer to the  $(1,0)$  direction above  $\delta \simeq 0.13$  which corresponds to the critical doping. Our dependence on doping of the direction resembles very much that found in a recent numerical work based on exact diagonalization within a dynamical mean-field theory in the Hubbard model [25] where the stable stripe phases move from a diagonal to a vertical configuration in the

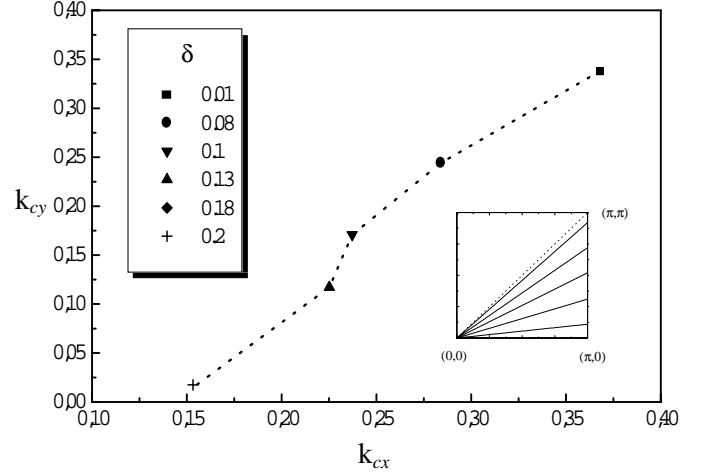


**Fig. 6.** Dependence of the components  $k_{cx}$  and  $k_{cy}$  on the doping  $\delta$  for the other values of parameters as in Figure 4. The inset shows the direction normal to the stripes at increasing doping starting from the diagonal.

range  $0.03 < \delta < 0.2$  at increasing doping. A similar behavior has been recently observed in NMR experiments on  $\text{La}_{2-x}\text{Sr}_x\text{CuO}_4$  [26,27] where a stripe structure has been detected in the Sr concentration region from  $x = 0.035$  to  $x = 0.25$  at low temperature. They found that the direction of the stripes changes from the diagonal direction on the  $\text{CuO}_2$  lattice in the spin glass composition ( $x = 0.02-0.05$ ) to vertical direction in the superconducting composition ( $x > 0.055$ ).

From the above analysis we conclude that the LRC forces introduce an order in the system rendering it similar to the case when spin fluctuations are present [8] even though the singularity appears at differently oriented momenta.

As in the previous case, we perform an analysis of the scattering amplitude close to the finite momentum divergence on the Fermi surface. The expansion of the denominator of (20) around  $\mathbf{k} = \mathbf{k}_c$  for  $\omega \sim 0$  gives

$$\Gamma^{\text{LR}}(\mathbf{k}, \omega) \sim -\frac{1}{\tilde{\Omega}(\mathbf{k}) - i\gamma\omega}, \quad (24)$$

where  $\tilde{\Omega}(\mathbf{k}_c) = 0$ . When  $\varepsilon_{\mathbf{q}} \neq \varepsilon_{\mathbf{k}_c+\mathbf{q}}$ , the coefficient  $\gamma$  is given by

$$\gamma(\mathbf{k} \sim \mathbf{k}_c, \omega \sim 0) = \pi \int \frac{d^2q}{(2\pi)^2} t_{\mathbf{k}_c+\mathbf{q}}^2 t_{\mathbf{q}}^2 \times \delta(\varepsilon_{\mathbf{q}}) \delta(\varepsilon_{\mathbf{q}} - \varepsilon_{\mathbf{k}_c+\mathbf{q}}) A_{\mathbf{q}} A_{\mathbf{k}_c+\mathbf{q}}. \quad (25)$$

On the line  $\varepsilon_{\mathbf{q}} = \varepsilon_{\mathbf{k}_c+\mathbf{q}}$  (which intersects the Fermi surface at the so-called *hot-spots*) the expression of  $\gamma$  is again given by equation (15) with  $\mathbf{k} \rightarrow \mathbf{k} - \mathbf{k}_c$ .

It should be noted that the imaginary term in (24) follows the behaviour of the mean-field fermionic bubble  $\propto \omega/k$  found previously, indicating that a RPA structure appears in the final result.

## 5 Conclusions

We have presented a strong-coupling analysis of the charge vertex function in the Hubbard model treated by means of a cumulant expansion method, where the effects of the strong Coulomb interaction are already taken into account at the zeroth order approximation. The results, based on a *generalized ladder-type* RPA show that the charge vertex becomes singular at a critical value of the doping for  $\omega = 0$  and  $\mathbf{k} = 0$ , implying the occurrence of a PS. The inclusion of long-range Coulomb interaction shifts the instability from  $\mathbf{k} = 0$  to  $\mathbf{k} = \mathbf{k}_c$ , leading to an incommensurate charge density wave type of instability. The stripes order has been investigated as a function of the Coulomb potential and the doping. We found that the stripes phase shows a crossover from diagonal to vertical stripes at increasing doping in the range  $0.01 \leq \delta \leq 0.2$ , accordingly to some dynamical mean-field calculations on the Hubbard model and recent NMR experiments on  $\text{La}_{2-x}\text{Sr}_x\text{CuO}_4$ . A similar behavior is observed at increasing  $U$ .

The consequences of the incommensurate charge density wave instability on the self-energy and the pseudogap formation in the single-particle spectra are under study. This analysis may be relevant for a microscopic understanding of the low-doping region of the high- $T_c$  cuprates, where a non-Fermi liquid behavior has been repeatedly observed.

The authors would like to thank Dr. A. Perali for useful discussions.

## References

1. T. Timusk, R.B. Tanner, in *Infrared Properties of High  $T_c$  superconductors*, Vol. 1, edited by M.G. Ginsberg (World Scientific, Singapore, 1988).
2. H. Takagi *et al.*, Phys. Rev. Lett. **69**, 2975 (1992).
3. Y. Ando *et al.*, Phys. Rev. Lett. **75**, 4622 (1995); Y. Ando *et al.*, Phys. Rev. Lett. **77**, 2065 (1996).
4. M.C. Schabel *et al.*, Phys. Rev. B **57**, 6090 and 6107 (1998).
5. M.R. Norman *et al.*, Nature **392**, 157 (1998).
6. H. Ding *et al.*, Phys. Rev. Lett. **78**, 2628 (1997).
7. S. Sachdev, J. Ye, Phys. Rev. Lett. **69**, 2411 (1992).
8. P. Montoux, A.V. Balatsky, D. Pines, Phys. Rev. B **46**, 14803 (1992); P. Montoux, D. Pines, Phys. Rev. B **50**, 16015 (1994).
9. C. Castellani, C. Di Castro, M. Grilli, Phys. Rev. Lett. **75**, 4650 (1995); C. Castellani, C. Di Castro, M. Grilli, Z. Phys. B **103**, 137 (1997).
10. J. Rossat-Mignod *et al.*, Physica B **186–189**, 1 (1993).
11. T.E. Mason *et al.*, Phys. Rev. Lett. **77**, 1604 (1996).
12. G.S. Boebinger *et al.*, Phys. Lett. **77**, 5417 (1996).
13. E.S. Bozin *et al.*, Phys. Rev. Lett. **84**, 5856 (2000).
14. J.M. Tranquada *et al.*, Phys. Rev. B **56**, 7689 (1996).
15. A. Bianconi *et al.*, Phys. Rev. Lett. **76**, 3412 (1996).
16. A. Bianconi *et al.*, Phys. Rev. B **54**, 4310 (1996).
17. V.A. Moskalenko, L.Z. Kon, Cond. Matt. Phys. **1**, 23 (1998).
18. W. Metzner, Phys. Rev. B **43**, 8549 (1991).
19. S. Pairault, D. Senechal, A.-M.S. Tremblay, Phys. Rev. Lett. **80**, 5389 (1998).
20. R. Citro, S. Di Matteo, M. Marinaro, K. Nakagawa, Physica B **281&282**, 814 (2000).
21. R. Citro, S. Di Matteo, M. Marinaro, Physica C **341–348**, 249 (2000).
22. F. Mancini, M. Marinaro, Y. Nakano, Physica B **159**, 330 (1989).
23. V.J. Emery, S.A. Kivelson, Physica C **209**, 597 (1993); U. Löw, V.J. Emery, K. Fabricius, S.A. Kivelson, Phys. Rev. Lett. **72**, 1918 (1994).
24. F. Becca, M. Tarquini, M. Grilli, C. Di Castro, Phys. Rev. B **54**, 12443 (1996).
25. M. Fleck *et al.*, Phys. Rev. Lett. **84**, 4962 (2000).
26. K. Yamada *et al.*, Phys. Rev. B **57**, 6165 (1998).
27. S. Wakimoto *et al.*, Phys. Rev. B **60**, 769 (1999); *ibid.* **61**, 3699 (2000).